Second-order time integration of the wave equation with dispersion correction procedures

Rune Mittet, EMGS

SUMMARY

Second-order time integration of the wave equation is numerically efficient with time steps close to the limit set by the stability criterion. However, the dispersion errors over realistic propagation distances are unacceptable with time steps in this range. A common procedure is to perform a post-propagation correction on the numerically simulated field. The post-propagation correction does not always provide a sufficiently accurate result. The reason is explained as a lacking source correction term. The proper source correction procedure is identified. Dispersion free results, using second-order time integration of the wave equation, can be achieved by applying a time-domain bivariate pre-propagation filter to all source time functions followed by a time-domain bivariate post-propagation filter to the simulated field at all recording positions. The bivariate pre-propagation filter and the bivariate post-propagation filter are valid for any reasonable simulation time step. The two filters can be calculated once since they are independent of the simulation time step and they can be applied with any modeling scheme that uses second order time integration.

INTRODUCTION

We are here dealing with correction methods for the time integration of the wave equation. The term wave equation should be understood in a wide sense. It can mean the Maxwell equations for loss-less propagation of electromagnetic fields or wave equations for acoustic and elastic seismic stress (pressure) and particle velocity fields. The time integration of the wave equation can be done with spectral accuracy as demonstrated by Tal-Ezer (1986) who introduced the Rapid Expansion Method (REM). However, for some applications, like for example reverse time migration (RTM), the REM method must be implemented in a time stepping manner as described by Pestana and Stoffa (2009, 2010) and by Tessmer (2011). An alternative to achieving spectral accuracy for the time stepping is to stay with the second order approximation, but perform proper dispersion correction procedures.

Spectral accuracy for the time integration was achieved in Mittet (2017) with a method that is due to Anderson et al. (2015). The formulation of Anderson et al. (2015) is the starting point also here. It will first be demonstrated that this formulation is equivalent to applying two frequency domain filters. One filter is to be applied to the source time function before time stepping is initiated. The second filter is to be applied on simulated fields after the time stepping has stopped. This approach have recently been derived by Koene et al. (2017) using an alternative derivation from the one given here.

The main result presented in this contribution is that the pre-propagation filter and the post-propagation filter have time domain representations that ensures both efficient design and efficient application. The two filters can be designed such that they are independent of the simulation time step. This is very convenient since only two filters need to be designed. Even if the filter design should take some computer time for large filters it does not matter since the filters can be used "forever" and for any modeling scheme based on second order time integration. The application of the filters are directly in the time domain so no complex numerical operations are required. This is in contrast to the frequency domain filters where both the pre- and the post-propagation filters require combinations of FFT's and DFT's. The application of the time domain filters are "mult-add" which is numerically very effective on most computers.

THEORY

Finite-difference simulations in media with variable material-parameter discontinuities are discussed in Mittet (2017). We are here dealing with the accuracy of the second-order time integration of the wave equation, thus to keep the error analysis as simple as possible a constant velocity model is used. Likewise, the wave propagation is assumed to be 1D. Generalization to inhomogeneous media and higher spatial dimensions is demonstrated for 2D acoustic and elastic simulations in Mittet (2017). Further examples of application of pre-propagation and post-propagation frequency domain filters are given in Koene et al. (2017).

The problem analyzed here has the generic form,

$$\frac{1}{c_0^2}\partial_t^2\sigma(z,t|z_s) - \partial_z^2\sigma(z,t|z_s) = \delta(z-z_s)S(t). \tag{1}$$

Here z gives the position of the field, σ. Further on, $\delta(z-z_s)$ is the Dirac distribution with z_s representing the source locations. The temporal behavior of the source is given by $S(t)$. The constant velocity is given by c_0. The spatial derivatives are performed with the pseudo-spectral method to achieve spectral accuracy in the space domain. A second-order temporal approximation to equation 1 is,

$$\frac{\sigma(z,t+\Delta t|z_s) - 2\sigma(z,t|z_s) + \sigma(z,t-\Delta t)|z_s)}{c_0^2(\Delta t)^2} - \partial_z^2\sigma(z,t|z_s) = \delta(z-z_s)S(t), \tag{2}$$

where Δt is the time step.

A temporal Fourier transform of equation 1 gives,

$$\frac{\omega^2}{c_0^2}\sigma(z,\omega|z_s) + \partial_z^2\sigma(z,\omega|z_s) = -\delta(z-z_s)S(\omega), \tag{3}$$

where the physicist convention for the temporal Fourier transform is used. A temporal Fourier transform of equation 2

10.1190/segam2018-2994778.1

gives,

$$\frac{\left(\frac{2}{\Delta t}\sin(\frac{\omega\Delta t}{2})\right)^2}{c_0^2}\sigma(z,\omega|z_s)+\partial_z^2\sigma(z,\omega|z_s)=-\delta(z-z_s)S(\omega) \quad (4)$$

or alternatively,

$$\frac{\omega^2}{c^2(\omega)}\sigma(z,\omega|z_s)+\partial_z^2\sigma(z,\omega|z_s)=-\delta(z-z_s)S(\omega), \quad (5)$$

with $c(\omega)=c_0\frac{\omega}{\left(\frac{2}{\Delta t}\sin(\frac{\omega\Delta t}{2})\right)}$.

The analytical solution to equation 3 is,

$$\sigma(z,\omega|z_s)=\tfrac{1}{2}c_0R(\omega)e^{i\frac{\omega}{c_0}(z-z_s)}, \quad (6)$$

for the case where $z>z_s$. In the time domain we have that $S(t)=\partial_tR(t)$. Since the time integration causes dispersion errors we need the solution to equation 5 in order to predict these errors. The solution is,

$$\sigma(z,\omega|z_s)=\tfrac{1}{2}c(\omega)R(\omega)e^{i\frac{\omega}{c(\omega)}(z-z_s)}. \quad (7)$$

We observe that there will be both amplitude errors and arrival-time errors present since the frequency dependent velocity multiplies the amplitude and appears in the argument.

Ideally I seek the solution to equation 1 but using a second-order approximation to the time derivative I end up with solutions to equation 2. If I use an alternative transform of equation 2,

$$\Psi(\omega')=\int_{-\infty}^{\infty}dt\Psi(t)e^{i\omega' t} \quad (8)$$

where,

$$\omega'=\frac{2}{\Delta t}\arcsin(\frac{\omega\Delta t}{2}) \quad \text{and} \quad \omega=\frac{2}{\Delta t}\sin(\frac{\omega'\Delta t}{2}), \quad (9)$$

then I end up with an equation identical to equation 4, but where ω is replaced by ω'. However, by application of equation 9,

$$\frac{\omega^2}{c_0^2}\sigma(z,\omega'|z_s)+\partial_z^2\sigma(z,\omega'|z_s)=-\delta(z-z_s)S(\omega'). \quad (10)$$

The field in the first term of equation 10 is now proportional to the desired squared wavenumber, but a remaining problem is that ω' is the frequency argument for the field and source term.

Some attention must be paid to the bandwidth by the introduction of ω'. With a given time step interval the maximum angular frequency is given as $\omega_{Nyq}=\pi/\Delta t$. However, due to the relation in equation 9 we require that the argument of the arcsin function is less than or equal to unity. Thus, the angular frequency limits are $-\frac{2}{\Delta t}\leq\omega\leq\frac{2}{\Delta t}$ and $-\frac{\pi}{\Delta t}\leq\omega'\leq\frac{\pi}{\Delta t}$. The integration limits for ω and ω' are then given by $\omega_c=\frac{2}{\Delta t}$, and $\omega_c'=\frac{\pi}{\Delta t}$.

It is shown in Mittet (2017) how an equation for the true solution, like equation 3, can be combined with an equation for the actual solution, like equation 10, to form a representation theorem. This representation theorem can be used to derive,

$$\sigma(z,\omega|z_s)=\frac{\sigma(z,\omega'|z_s)S(\omega)}{S(\omega')}, \quad (11)$$

which is the expression given in Anderson et al. (2015) and also used in Mittet (2017) for temporal dispersion corrections.

The dispersion correction procedure is then to apply the transform in equation 8 with the frequency as given by equation 9 to the simulated field and to the source waveform. In addition, the standard Fourier transform must be applied to the source waveform. Equation 11 can then be applied, followed by the standard inverse Fourier transform,

$$\sigma(z,t|z_s)=\frac{1}{2\pi}\int_{-\omega_c}^{\omega_c}d\omega\ \sigma(z,\omega|z_s)e^{-i\omega t}. \quad (12)$$

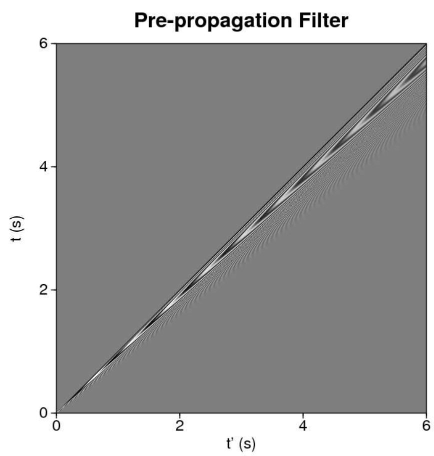

Figure 1: Pre-propagation filter. To be applied to sources for simulations with arbitrary temporal step length. Here a 1 ms step length is used for illustration. The dimensionless parameter θ' runs from 0.0 to 12000.0 along the abscissa.The dimensionless parameter θ runs from 0.0 to 12000.0 along the ordinate

Wang and Xu (2015) and also Koene and Robertsson (2017) proposed to perform the dispersion correction by the following procedure on the numerically simulated field, $\hat{\sigma}(z,t|z_s)$,

$$\sigma(z,t|z_s)=\frac{1}{(2\pi)}\int_{-\omega_c}^{\omega_c}d\omega e^{-i\omega t}\int_0^{T_{Max}}dt'\hat{\sigma}(z,t|z_s)e^{i\omega' t'}. \quad (13)$$

This dispersion correction procedure is identical to the one described above if the source function ratio in equation 11 is set to unity, thus using,

$$\sigma(z,\omega|z_s)=\sigma(z,\omega'|z_s). \quad (14)$$

The problem with equation 13 is that this is only a partial dispersion correction procedure. The situation is that a frequency dependent amplitude and phase error still remains in the numerically simulated fields after the application of this dispersion correction procedure. For some situation this remaining error is unacceptably large.

Note that if the ratio of the source waveforms in equation 11 is unity, then the transform proposed by Wang and Xu (2015) and Koene and Robertsson (2017) is applicable. To achieve a source waveform ratio equal to unity for all frequencies I postulate a source time function for the numerical simulation, $\tilde{S}(t)$, related to the desired source function, $S(t)$, by,

$$\tilde{S}(\omega') = S(\omega), \tag{15}$$

such that,

$$\begin{aligned}\tilde{S}(t) &= \frac{1}{2\pi}\int_{-\omega_c'}^{\omega_c'} d\omega' e^{-i\omega' t}\tilde{S}(\omega') = \frac{1}{2\pi}\int_{-\omega_c'}^{\omega_c'} d\omega' e^{-i\omega' t} S(\omega) \\ &= \frac{1}{2\pi}\int_{-\omega_c'}^{\omega_c'} d\omega' e^{-i\omega' t}\int_0^{T_{Max}} dt' S(t') e^{i\omega t'}. \end{aligned} \tag{16}$$

The source waveforms are transformed according to equation 16 prior to initiating the numerical simulation. The correction procedure described by equation 13 is then performed after the numerical simulation has ended. This result is here a direct consequence of the relation in equation 11 due to Anderson et al. (2015) but it can also be derived by an alternative approach as showed Koene et al. (2017).

A bivariate source filter can be calculated based on equation 16,

$$\mathscr{F}_S(t,t') = \frac{1}{2\pi}\int_{-\omega_c'}^{\omega_c'} d\omega' e^{-i(\omega' t - \omega t')}, \tag{17}$$

and this filter is applied to all source time functions, $S(t|z_s)$, as a pre-propagation correction in the following manner,

$$\tilde{S}(t|z_s) = \int_0^{T_{Max}} dt' \mathscr{F}_S(t,t') S(t'|z_s). \tag{18}$$

Such a bivariate filter is shown in Figure 1.

A bivariate wavefield filter for post-propagation corrections can be constructed in the same manner. From equation 13 we obtain,

$$\mathscr{F}_W(t,t') = \frac{1}{2\pi}\int_{-\omega_c}^{\omega_c} d\omega e^{i(\omega' t' - \omega t)}. \tag{19}$$

This filter is applied to the numerically simulated field, $\hat{\sigma}(z,t|z_s)$, as a post-propagation correction,

$$\sigma(z,t|z_s) = \int_0^{T_{Max}} dt' \mathscr{F}_W(t,t')\hat{\sigma}(z,t'|z_s). \tag{20}$$

The post-propagation filter is shown in Figure 2.

For practical calculations we can express the two filters as,

$$\begin{aligned}\mathscr{F}_S(t,t') &= \frac{1}{\pi}\int_0^{\omega_c'} d\omega' \cos\left(\omega_c \sin(\frac{\omega'}{\omega_c})t' - \omega' t\right), \\ \mathscr{F}_W(t,t') &= \frac{1}{\pi}\int_0^{\omega_c} d\omega \cos\left(\omega_c \arcsin(\frac{\omega}{\omega_c})t' - \omega t\right). \end{aligned} \tag{21}$$

Both $\mathscr{F}_S(t,t')$ and $\mathscr{F}_W(t,t')$ are independent of the source time function and the numerically simulated field. In the form given in equation 21 it appears as if the filters depend on the time

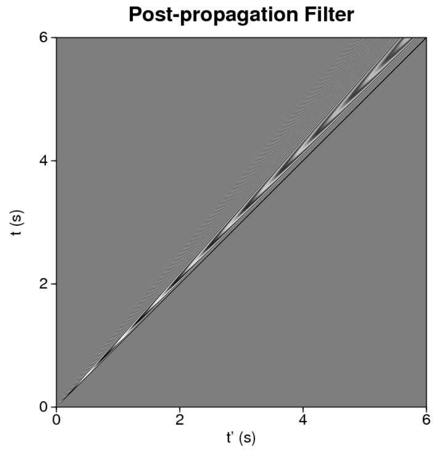

Figure 2: Post-propagation filter. To be applied to recorded fields for simulations with arbitrary temporal step length. Here a 1 ms step length is used for illustration

step, Δt. It will be a major drawback if a new filter must be designed as soon as the the time step change. However, with a proper sampling it turns out that only one $\mathscr{F}_S(t,t')$ filter is required, valid for any Δt. Likewise, only one $\mathscr{F}_W(t,t')$ filter is required, also valid for any Δt. To see this, we first change the integration variables, $\omega' = \eta\omega_c$ in the upper equation 21 and $\omega = \eta\omega_c$ in the lower equation 21. Also use $\theta' = \omega_c t'$ and $\theta = \omega_c t$ for the upper equation 21 and $\theta' = \omega_c t'$ and $\theta = \omega_c t$ for the lower equation 21. Equation 21 is then,

$$\begin{aligned}\mathscr{F}_S(\theta,\theta') &= \frac{\omega_c}{\pi}\int_0^{\frac{\pi}{2}} d\eta \cos\left(\sin(\eta)\theta' - \eta\theta\right), \\ \mathscr{F}_W(\theta,\theta') &= \frac{\omega_c}{\pi}\int_0^{1} d\eta \cos\left(\arcsin(\eta)\theta' - \eta\theta\right), \end{aligned} \tag{22}$$

where we can write $\mathscr{F}_S(t(\theta),t'(\theta')) = \mathscr{F}_S(\theta,\theta')$ for the pre-propagation filter and $\mathscr{F}_W(t(\theta),t'(\theta')) = \mathscr{F}_W(\theta,\theta')$ for the post-propagation filter. First we replace, $\omega_c = 2/\Delta t$, with 2. This since the discrete versions of the integrals in equations 18 and 20 have multiplication with Δt. If we replace $\omega_c = 2/\Delta t$, with 2, then multiplication with Δt when applying the filters is no longer required. Note that $\theta' = \frac{2t'}{\Delta t}$ and $\theta = \frac{2t}{\Delta t}$. Let both t' and t be sampled every Δt, such that $t' = n'\Delta t$ and $t = n\Delta t$, where n' and n take on the integer values $0,1,2,3,4,\ldots$. The maximum times are given by $n' = n = N_T$. We then have $\theta_{n'} = 2n'$ and $\theta_n = 2n$ such that $\theta_{n'}$ and θ_n will take on the real values $0.0, 2.0, 4.0, 6.0, \ldots$ when calculating the filters.

The integral over η is performed with a step length,

$$\Delta\eta = \frac{\Delta\omega}{\omega_c} = \frac{\frac{2\pi}{N_t\Delta t}}{\frac{2}{\Delta t}} = \frac{\pi}{N_T}, \tag{23}$$

and with $N_\eta = 1/\Delta\eta$ and $N_\eta' = \frac{\pi}{2}/\Delta\eta$. Using $\eta^m = m\Delta\eta$ the

10.1190/segam2018-2994778.1

filters are generated by,

$$\mathscr{F}_S(\theta_n,\theta_{n'}) = \frac{2\Delta\eta}{\pi}\sum_{m=0}^{N'_\eta}\cos\left(\sin(\eta^m)\theta_{n'} - \eta^m\theta_n\right),$$

$$\mathscr{F}_W(\theta_n,\theta_{n'}) = \frac{2\Delta\eta}{\pi}\sum_{m=0}^{N_\eta}\cos\left(\arcsin(\eta^m)\theta_{n'} - \eta^m\theta_n\right). \quad (24)$$

Observe that Δt does not need to be specified with the given sampling of θ and θ'. The filters are in principle valid for any simulation time step. The filters are applied as,

$$\begin{aligned}\tilde{S}(n\Delta t|z_s) &= \sum_{n'=0}^{N_T}\mathscr{F}_S(\theta_n,\theta_{n'})S(n'\Delta t,z_s),\\ \sigma(z,n\Delta t|z_s) &= \sum_{n'=0}^{N_T}\mathscr{F}_W(\theta_n,\theta_{n'})\hat{\sigma}(z,n'\Delta t|z_s).\end{aligned} \quad (25)$$

We have that $t_n = \frac{1}{2}\theta_n\Delta t = n\Delta t$ and $t_{n'} = \frac{1}{2}\theta_{n'}\Delta t = n'\Delta t$ so equation 25 is,

$$\begin{aligned}\tilde{S}(t_n|z_s) &= \sum_{n'=0}^{N_T}\mathscr{F}_S(t_n,t_{n'})S(t_{n'},z_s),\\ \sigma(z,t_n|z_s) &= \sum_{n'=0}^{N_T}\mathscr{F}_W(t_n,t_{n'})\hat{\sigma}(z,t_{n'}|z_s),\end{aligned} \quad (26)$$

as desired. The dispersion correction procedure is then to apply $\mathscr{F}_S$ to all source functions prior to the modeling. After the modeling has completed the modeled data is filtered with $\mathscr{F}_W$.

One limitation of the filters is that they can only be applied to time functions of length $T_{Max} \leq N_T\Delta t$. Hence, it is advantageous to design filters with a large N_T. This may actually require some computer time. However, each filter needs only be calculated once. For the future they can be used for almost any simulation independent of the time step. If for example $N_T = 10000$ then the filters can be used for traces of up to 10 s with a 1 ms simulation time step and traces of up to 20 s if the simulation time step is 2 ms. For example, a filter with $N_T = 30000$ will be 3.6 GB in size without compression ($4 \times N_T \times N_T$). If this filter is designed, then smaller and more handy filters can be extracted as subsets of that main filter. An extracted $N_T = 10000$ filter will be 400 MB without compression.

The application of the filters are directly in the time domain so no complex numerical operations are required. This is in contrast to the frequency domain filters where both the pre- and the post-propagation filters require combinations of FFT's and DFT's. The application of the time domain filters are easily vectorized on most computers.

RESULTS

An example of applying the pre-propagation and post-propagation filters are shown in Figure 3. The modeling is performed in a whole-space with velocity 1500 m/s and the total propagation distance, Z_{rs}, is 6000 m. The maximum frequency of the field is 100 Hz with a peak frequency at 40 Hz. The phase and amplitude errors are displayed as a function of frequency. Equation 7 is divided by equation 6. The relative error in amplitude is $\varepsilon_A = \frac{c(\omega)}{c_0} - 1$ and the equivalent traveltime error is $\Delta\tau = Z_{rs}(1/c(\omega) - 1/c_0)$ as explained in Mittet (2017). It is obvious that errors are large over 6000 m propagation distance. Traveltime errors are frequency dependent and exceed 1 ms already for the 10 Hz component of the field. Excellent results are achieved with the application of the pre-propagation and post-propagation filters.

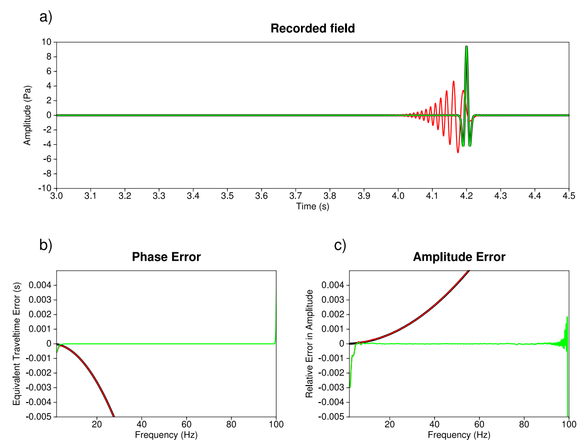

Figure 3: a) Field amplitudes, the black curve is the analytical solution, the red curve is the uncorrected finite-difference solution. The green curve is the corrected finite-difference solution. b) Phase error given as a traveltime error. The black curve is the dispersion error predicted by theory. The red curve is the dispersion error measured on the uncorrected simulated field. The green curve is the dispersion error measured on the corrected simulated field. c) Relative amplitude error. The black curve is the amplitude error predicted by theory. The red curve is the amplitude error measured on the uncorrected simulated field. The green curve is the amplitude error measured on the corrected simulated field.

CONCLUSIONS

Both the phase and amplitude errors introduced by the second order accurate time integration can be removed by proper correction procedures. It is not sufficient to perform only a post-propagation correction on the numerically simulated field. Pre-propagation correction on the source time functions must be applied in order to achieve acceptable results.

The time-domain bivariate pre-propagation filter and the time-domain bivariate post-propagation filter are valid for any reasonable simulation time step. They can be calculated once and then used for any modeling scheme that uses second order time stepping.

10.1190/segam2018-2994778.1

REFERENCES

Anderson, J., E. V. Brytik, and G. Ayeni, 2015, Numerical temporal dispersion corrections for broadband temporal simulation, RTM and FWI: Presented at the 58th Annual International Meeting, SEG, Expanded Abstracts, 1096–1100, https://doi.org/10.1190/segam2015-5817144.1.

Fornberg, B., 1975, On a Fourier method for the integration of hyperbolic equations: SIAM Journal on Numerical Analysis, 509–528.

Gazdag, J., 1981, Modeling of the acoustic wave equation with transform methods: Geophysics, **46**, 854–859, https://doi.org/10.1190/1.1441223.

Koene, E., and J. Robertsson, 2017, Removing numerical dispersion artifacts from reverse time migration and full-waveform inversion: 87th Annual International Meeting, SEG, Expanded Abstracts, 4143–4147, https://doi.org/10.1190/segam2017-17631589.1.

Koene, E. F., J. O. Robertsson, F. Broggini, and F. Andersson, 2017, Eliminating time dispersion from seismic wave modeling: Geophysical Journal International, 169–180.

Kosloff, D., and E. Baysal, 1982, Forward modeling by a Fourier method: Geophysics, **47**, 1402–1412, https://doi.org/10.1190/1.1441288.

Kreiss, H. O., and J. Oliger 1972, Comparison of accurate methods for the integration of hyperbolic equations: Tellus, **24**, 199–215, https://doi.org/10.3402/tellusa.v24i3.10634.

Mittet, R., 2017, On the internal interfaces in finite-difference schemes: Geophysics, **82**, no. 4, T159–T182, https://doi.org/10.1190/geo2016-0477.1.

Pestana, R. C., and P. L. Stoffa, 2009, Rapid expansion method (REM) for time-stepping in reverse time migration (RTM): 79th Annual International Meeting, SEG, Expanded Abstracts, 2819–2823, https://doi.org/10.1190/1.3255434.

Pestana, R. C., and P. L. Stoffa, 2010, Time evolution of the wave equation using rapid expansion method: Geophysics, **75**, no. 4, T121–T131, https://doi.org/10.1190/1.3449091.

Tal-Ezer, H., 1986, Spectral methods in time for hyperbolic equations: SIAM Journal on Numerical Analysis, **23**, 11–26, https://doi.org/10.1137/0723002.

Tessmer, E., 2011, Using the rapid expansion method for accurate time-stepping in modeling and reverse-time migration. Geophysics, **76**, no. 4, S177–S185, https://doi.org/10.1190/1.3587217.

Wang, M., and S. Xu, 2015, Finite-difference time dispersion transforms for wave propagation: Geophysics, **80**, no. 6, WD19–WD25, https://doi.org/10.1190/geo2015-0059.1.

10.1190/segam2018-2994778.1